

Supporting Information

Thin Solid Electrolyte Layers Enabled by Nanoscopic Polymer Binding

Yejing Li¹, Xuefeng Wang¹, Hongyao Zhou¹, Xing Xing¹, Abhik Banerjee¹, John Holoubek¹, Haodong

Liu¹, Ying Shirley Meng^{1, 2}, and Ping Liu^{1, 2*}

¹ *Department of NanoEngineering, University of California San Diego, La Jolla, CA 92093, USA*

² *Sustainable Power and Energy Center, University of California, San Diego, La Jolla, CA 92093, USA*

**Corresponding author.*

E-mail address: piliu@eng.ucsd.edu

Experimental details

1. Synthesis of solid electrolyte-in-polymer matrix (SEPM), cathode and anode materials

All material synthesis, cell fabrication, and testing were performed inside a glove box (MBRAUN MB 200B, H₂O < 0.5 ppm, O₂ < 0.5 ppm). All the precursors for SEPM fabrication were finely grounded and the solvent was dehydrated with molecular sieves before use. The high purity Li₂S (99.98%, Sigma-Aldrich) and S (Sigma-Aldrich) precursors were dissolved in THF (Sigma-Aldrich) and stirred for 12 hours. Then, a stoichiometric ratio of P₂S₅ (99%, Sigma-Aldrich) was added to the above solution and stirred 24 hours, forming an LPS_S suspension. Separately, ES (Sigma-Aldrich) was dissolved in THF and stirred overnight, forming the ES_THF solution. A certain percentage of the ES_THF solution was added to the LPS_S suspension followed by 24 hours mixing, forming an LPS_S_PES suspension. The above suspension was first dried in the furnace in the glovebox for 24 hours at 140 °C and then transferred to a vacuum oven to further THF evaporation for 48 hours at 140 °C. The free-standing SEPM@Kevlar film was also fabricated via a solution method. The mixed LPS_S_PES suspension was dropped on to a Kevlar mat followed by the

above drying process. After that, the dried SEPM@Kevlar pellet was pressed under a pressure of 200 MPa forming the free-standing SEPM@Kevlar film.

A solution method was employed to coat LiNbO_3 (LNO) on NCA particles. First, lithium ethoxide (99.8 %, Sigma-Aldrich) and niobium ethoxide (99%, Sigma-Aldrich) were dissolved in dry ethanol (99.8%, Sigma-Aldrich). NCA powder was then added into the solution and stirred for one hour. The dried powder was collected by evaporating the ethanol using a rotary evaporator followed by heat-treatment of the powder at 450 °C for one hour, yielding LNO coated NCA. The coated powder was dried overnight at 100 °C under vacuum before transferring to the inside of the glove box for storage and fabrication of solid-state batteries.

The $\text{Li}_{0.5}\text{In}$ alloy anode was prepared by mixing the stoichiometric amount of lithium powder (FMC) and indium powder (99.6%, Alfa Aesar) for 20 mins in a vortex mixer.

2. Characterization

To analyze the synthesized SEPM, all characterizations were conducted carefully without any air exposure. X-ray diffraction (XRD, Bruker, D2 Phaser) with $\text{Cu K}\alpha$ radiation was used to analyze the structure of the SEPM. The morphology and the thickness of the as-prepared SEPM were collected from scanning electron microscopy (SEM, FEI Quanta 250) operating at 10 kV. Bonding environments of the SEPM were investigated by Raman spectroscopy (Perkin Elmer, Raman station 400F) and Fourier transform infrared spectroscopy (FTIR, Perkin Elmer, Spectrum 100 FTIR) in the ATR mode. X-ray photon spectroscopy (XPS, Kratos Ultra DLD) was performed to investigate the chemical environments of the SEPM. All spectra were calibrated with C 1s (284.8 eV) for adventitious carbon in the chamber. All XPS measurements were collected with a 300 μm to 700 μm spot size. Survey scans were collected with a 1.0 eV resolution from 0 to 1200 eV, followed by high-resolution 0.1 eV, 1 s scans of the Li 1s, C 1s, P 2p, and S 2p regions. The spectra were analyzed by Avantage (Thermal Scientific) software. Transmission electron microscopy (TEM) was recorded on a field emission gun JEOL-2800 at 200 kV with Gatan OneView Camera (full 4 K * 4 K

resolution) at -180 °C. The sample loading and transferring were carried in a home-made glovebox purging with pure Ar, which minimized any air exposure. Scanning transmission electron microscopy/energy dispersive X-ray spectroscopy (STEM/EDX) was performed on primary particles at an annular dark field (ADF) mode with a beam size of ~0.5 Å.

3. Electrochemical analysis

Impedance spectra were measured using electrochemical impedance spectroscopy (EIS, BioLogic, VMP-300t) in a frequency range from 7 MHz to 1 MHz. SEPM pellets was prepared by cold pressing in a Swagelok type cell with a Ti||SEPM||Ti configuration.

The cathode composites were prepared with 10 mg NCA, 11 mg SEPM and 0.8 mg carbon as the electronically conductive additive. All components were hand ground with an agate mortar to make a homogeneous mixture. The SEPM was pressed with 360 MPa pressure to make the pellet. 10 mg of the cathode composite was pressed on top of the SEPM with the same pressure. Finally, 70 mg of the $\text{Li}_{0.5}\text{In}$ alloy was pressed with 100 MPa pressure on the other side of the SEPM. All the procedures were performed in a polyaryletheretherketone (PEEK) mold (diameter = 13 mm) with two Ti metal rods as current collectors. The all-solid-state batteries were evaluated at a static pressure of 25 MPa.

4. Porosity calculation

Since the sulfide-based SPEM sample is sensitive to air and moisture, it is difficult to use the conventional method of weighing to measure the porosity. Alternatively, we can estimate the porosity based on the density and weight of each component in the SPEM composite. The total mass for the SEPM@Kevlar film is 13.2 mg. For the Kevlar, the density and the corresponding mass (1.33 cm^2) is 1.44 g/cm^3 and 1.4 mg. The mass for the SEPM is 11.8 mg. In addition, the density of the Li_3PS_4 , S and PES is 1.87 g/cm^3 , 2 g/cm^3 , and 1.34 g/cm^3 , respectively. Based on the thermogravimetric analysis, the mass ratio for the Li_3PS_4 , S and PES is 65:15:20. Thus, the average density for the SEPM is 1.7835 g/cm^3 . The theoretical volume for SEPM (V_t) $V=m/\rho=11.8/1.7835=6.62 \times 10^{-3} \text{ (cm}^3\text{)}$. The area of the SEPM is $S = \pi r^2 = \pi \times 0.65^2 = 1.33 \text{ cm}^2$.

The thickness of the SE is 60 μm as shown in Figure 8f. Then the practical total volume $V = S \times h = 1.33 \times 60 \times 10^{-4} = 7.98 \times 10^{-3} (\text{cm}^3)$. The volume for the Kevlar mat is $9.7 \times 10^{-4} (\text{cm}^3)$. The practical volume for SEPM (V_p) is $7.01 \times 10^{-3} (\text{cm}^3)$.

Thus, the porosity $p = (V_p - V_t / V_p) \times \% = 5.6\%$.

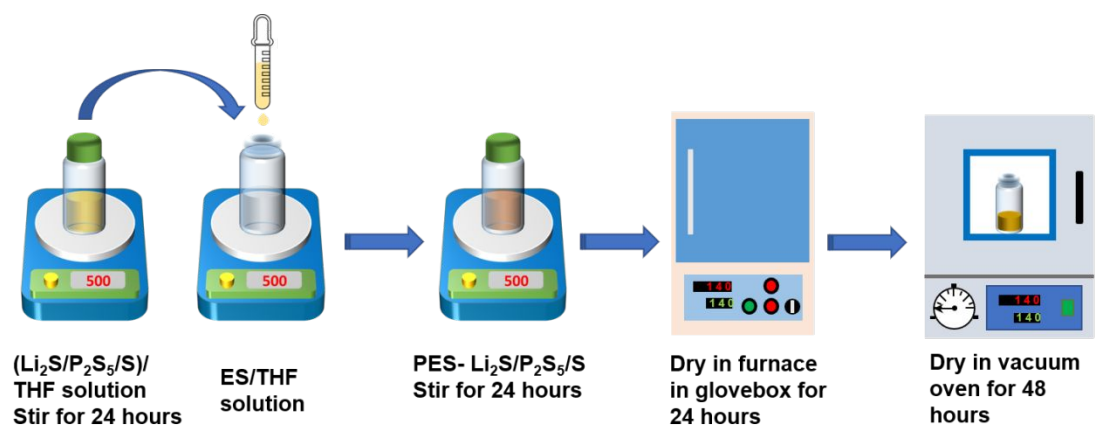


Figure S1. Schematic processes for the synthesis of the $\beta\text{-Li}_3\text{PS}_4\text{-S-PES}$ solid electrolyte.

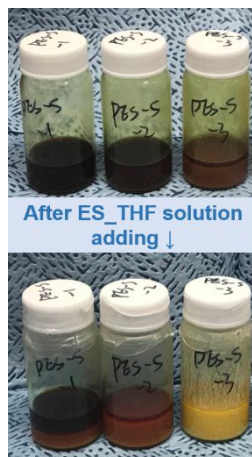


Figure S2. The color changes for the solution before and after the ES_THF solution. The composition in the solution was listed in the Table S2. From left to right, the sulfur content was decreased.

Table S1. Content ratio of β -Li₃PS₄, S, and PES in the SEPM.

	PES_ES_1	PES_ES_2	PES_ES_3
ES	0.75 mmol	1.5 mmol	3.0 mmol
Li ₂ S	2.5 mmol	2.5 mmol	2.5 mmol
P ₂ S ₅	0.83 mmol	0.83 mmol	0.83 mmol
S	5 mmol	5 mmol	5 mmol
S/Li ₂ S	2	2	2

Table S2. Content ratio of β -Li₃PS₄, S, and PES in the SEPM.

	PES_S_1	PES_S_2	PES_S_3
ES	1.5 mmol	1.5 mmol	1.5 mmol
Li ₂ S	2.5 mmol	2.5 mmol	2.5 mmol
P ₂ S ₅	0.83 mmol	0.83 mmol	0.83 mmol
S	5 mmol	4 mmol	3 mmol
S/Li ₂ S	2	1.6	1.2

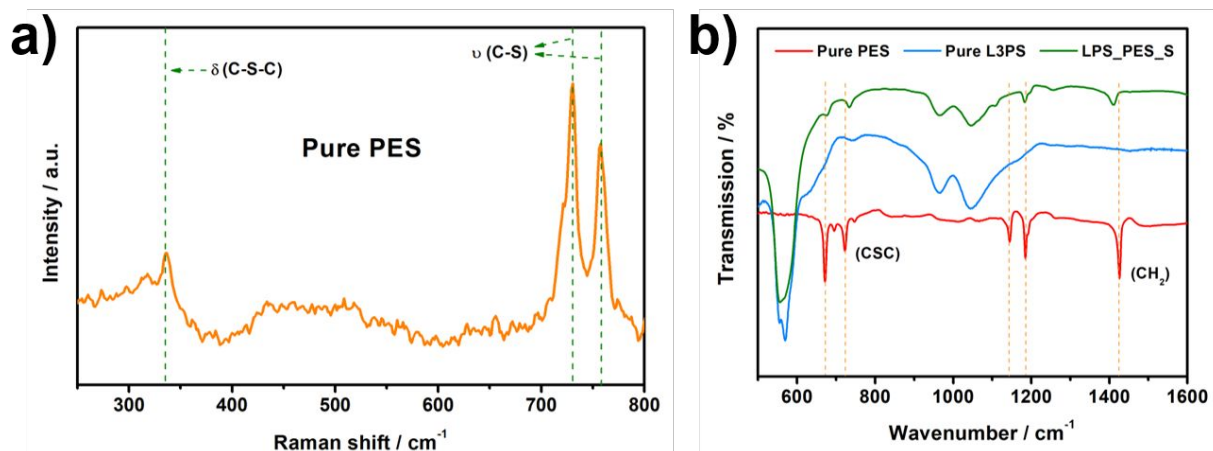


Figure S3. Raman and FTIR spectra of pure Li_3PS_4 _S and PES synthesized by the solution method.

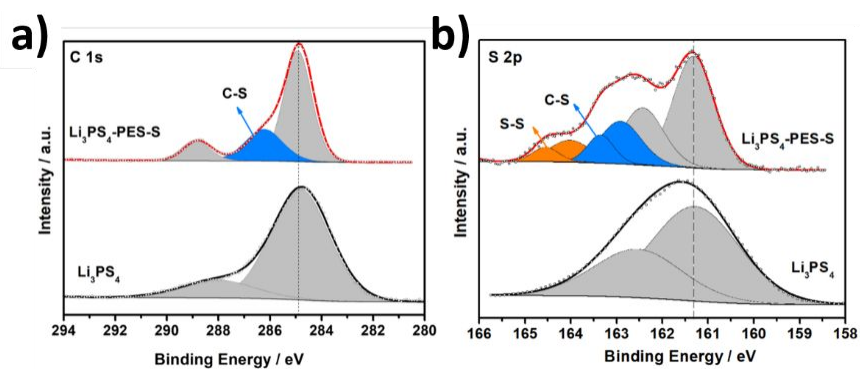


Figure S4. XPS spectra of C1s (a) and S2p (b) for pure PES (red) $\text{Li}_3\text{PS}_{4+x}$ (blue) and SPEM composite.

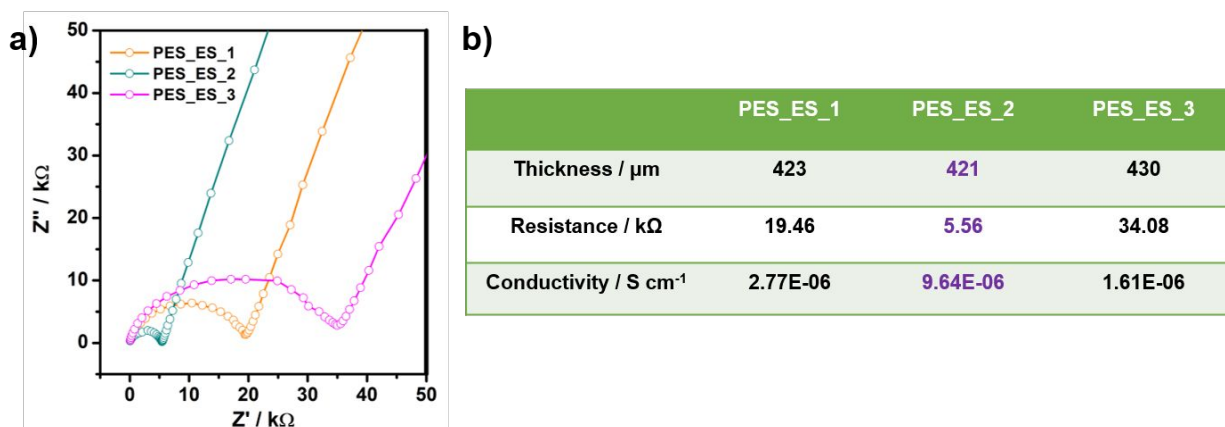


Figure S5. Nyquist plots (a) for the SEPM with varying ES content and the corresponding ionic conductivity

(b) calculated based on the equation $\rho = \frac{l}{RA}$ (l: thickness; R: resistance, A: area).

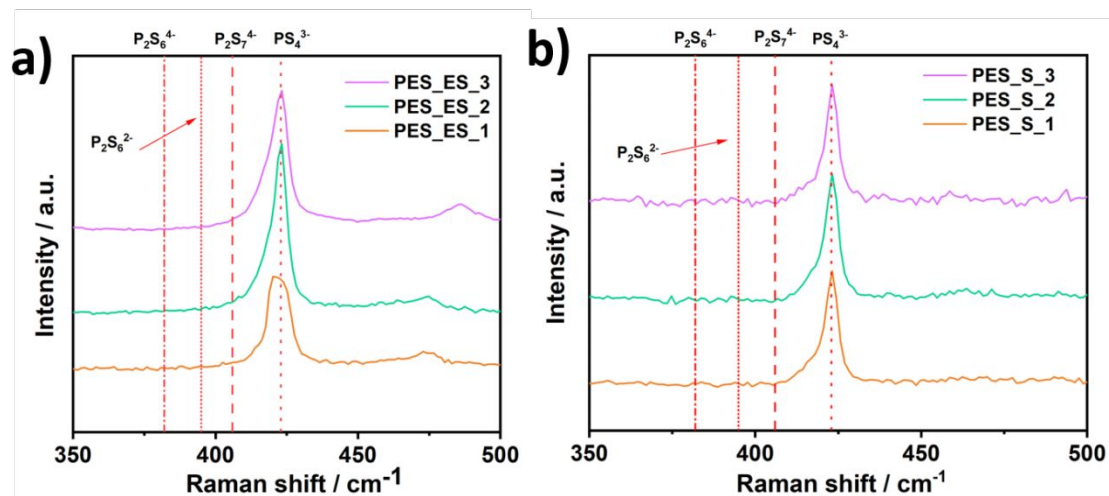


Figure S6. The zoomed-in region of Raman spectra of SPEM composite with different ES content (a) and S content (b).

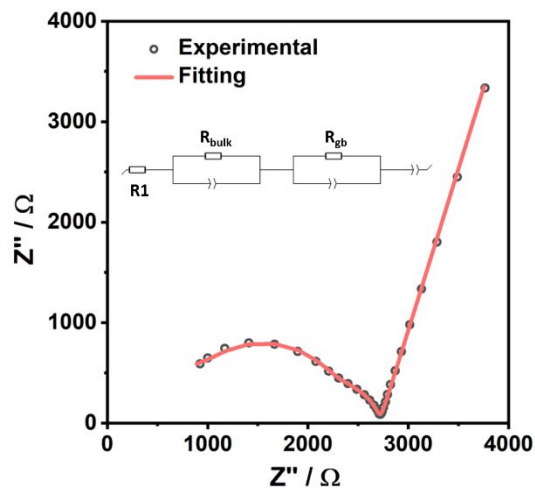


Figure S7. The experimental and the fitting data of the Nyquist plot for sample PES_S_2. The inset is the equivalent circuit used for fitting. R_1 is the resistance for the external circuit, R_{bulk} is the bulk resistance and R_{gb} is the resistance for the grain boundary.

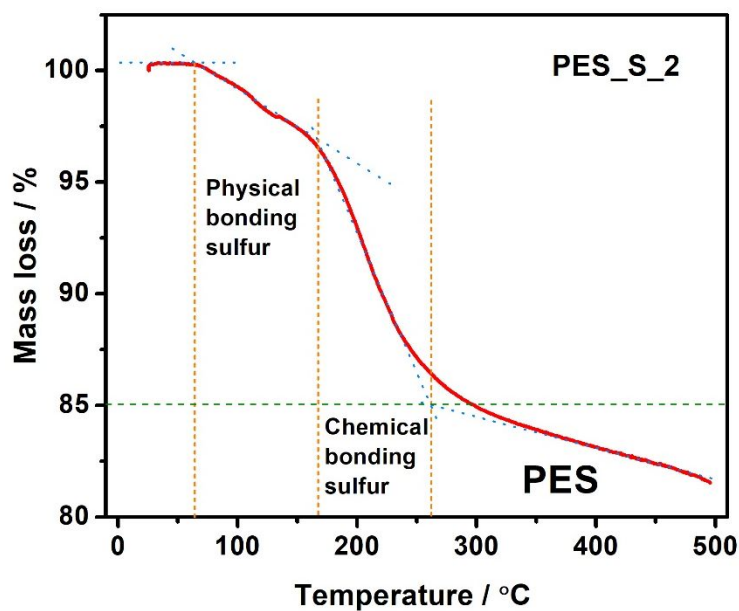


Figure S8. Thermogravimetric analysis of the PES_S_2 sample.

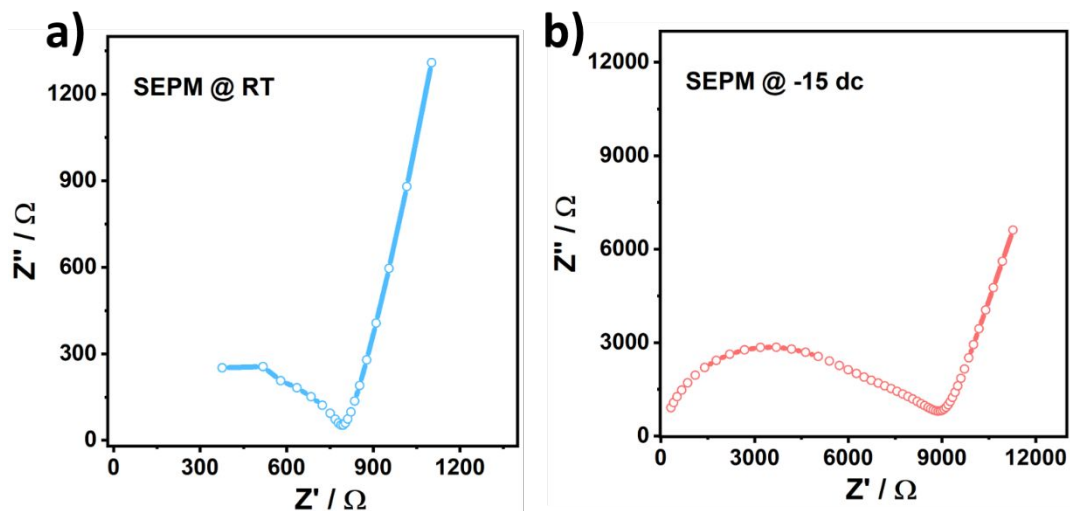


Figure S9. The Nyquist plots for the SEPM tested at room temperature (25 °C) (a) and -15 °C (b).

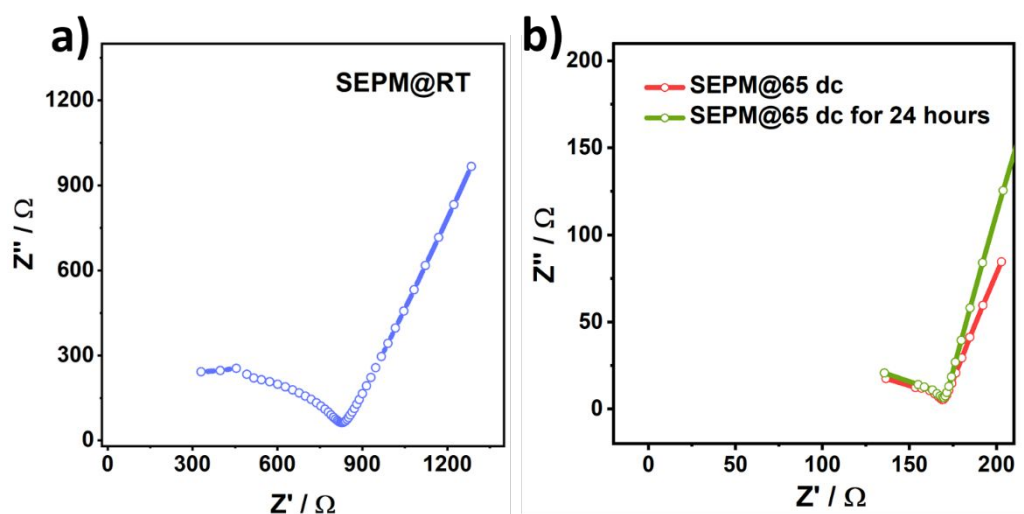


Figure S10. The Nyquist plots for the SEPM tested at room temperature (25 °C) (a), 65 °C for 4 hours and 65 °C for 24 hours (b).

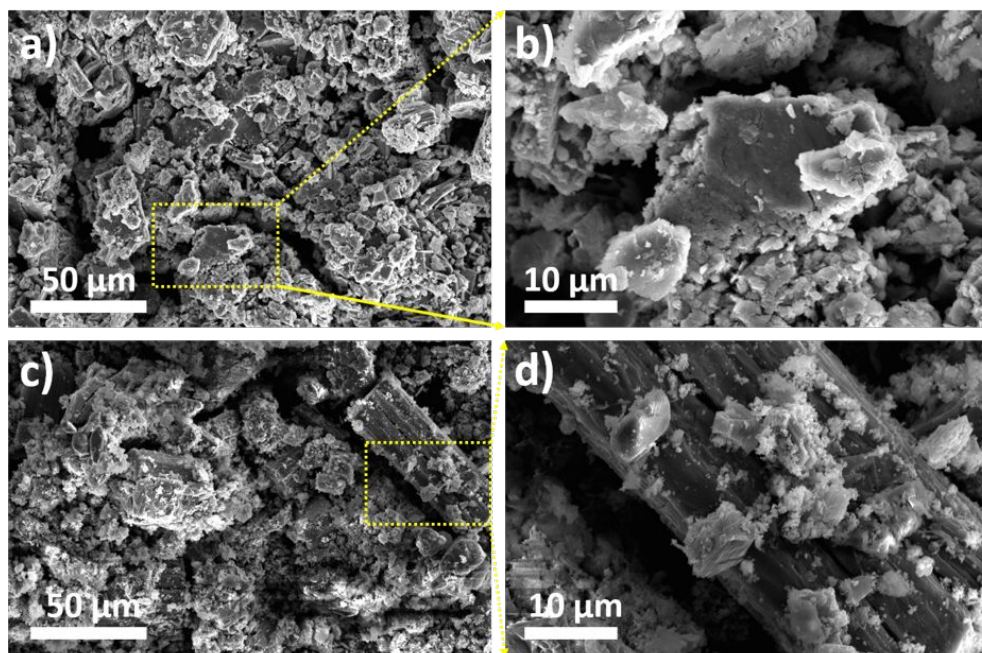


Figure S11. Morphological (a-d) SEM comparison between in-situ formed (a and b) and physical blended (c and d) β - Li_3PS_4 -S-PES SEPM.

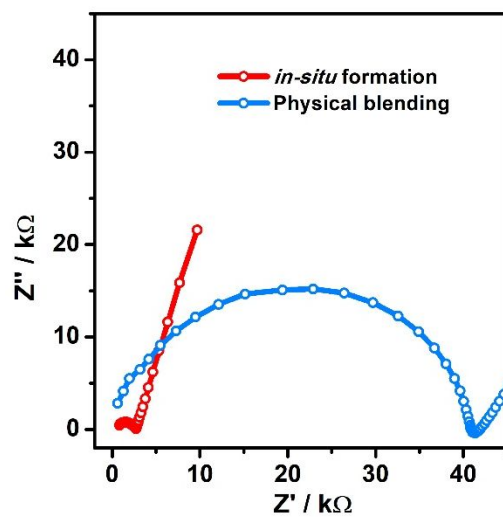


Figure S12. EIS spectra of LPS-S-PES composites prepared by physical blending and in-situ formation.

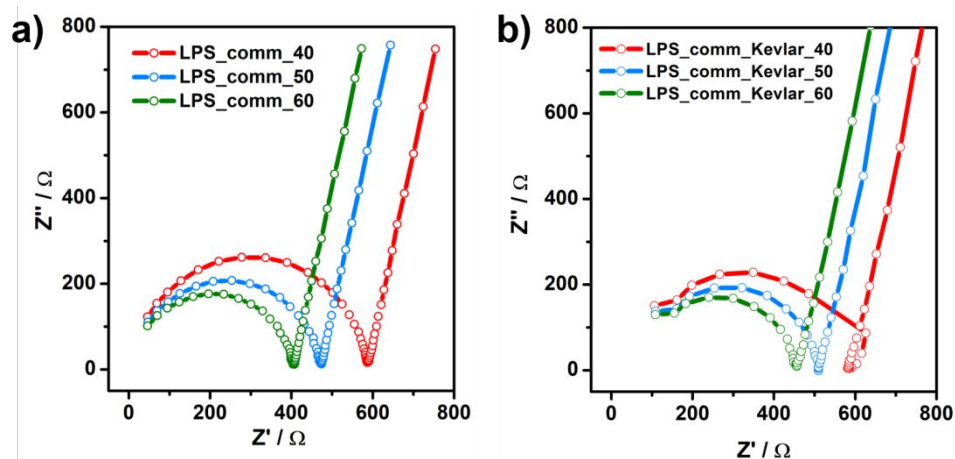


Figure S13. Nyquist plots of the commercial β - Li_3PS_4 without (a) and with (b) Kevlar mat under different pressure.

Table S3. Summary of activation energy for the reported sulfide-based electrolyte.

Materials	Activation energy / kJ/mol	Reference
$\text{Li}_3\text{PS}_4/\text{S}/\text{PES}$	39.42	This paper
$\text{PEO}/\text{Li}_3\text{PS}_4$	110-124	Chen, S., et al. (2018). Journal of Power Sources 387: 72-80. ¹
$80\text{Li}_2\text{S} \cdot 20\text{P}_2\text{S}_5$	40-43	Sakuda, A., et al. (2010). Journal of the American Ceramic Society 93(3): 765-768. ²
$x\text{Li}_2\text{S} \cdot (100-x)\text{P}_2\text{S}_5$ electrolytes	39	Zhang, Y., et al. (2017). Solid State Ionics 305: 1-6. ³
Li_3PS_4	47.12	Tachez, M., et al. (1984). Solid State Ionics 14(3): 181-185. ⁴
Nanoporous β - Li_3PS_4	34.23	Liu, Z., et al. (2013). Journal of the American Chemical Society 135(3): 975-978. ⁵
Li_3PS_4	31	Phuc, N. H. H., et al. (2016). Solid State Ionics 288: 240-243. ⁶

Li ₃ PS ₄ /Methyl-imine		Whiteley, J. M., et al. (2015). "Ultra-thin Solid-State Li-Ion Electrolyte Membrane Facilitated by a Self-Healing Polymer Matrix." Advanced Materials 27(43): 6922-6927. ⁷
Li ₃ PS ₄	41.9	Yamada, T., et al. (2015). Journal of the Electrochemical Society 162(4): A646-A651. ⁸

Reference:

1. Chen, S.; Wang, J.; Zhang, Z.; Wu, L.; Yao, L.; Wei, Z.; Deng, Y.; Xie, D.; Yao, X.; Xu, X., In-situ preparation of poly(ethylene oxide)/Li₃PS₄ hybrid polymer electrolyte with good nanofiller distribution for rechargeable solid-state lithium batteries. *J. Power Sources* **2018**, *387*, 72-80.
2. Sakuda, A.; Hayashi, A.; Hama, S.; Tatsumisago, M., Preparation of Highly Lithium-Ion Conductive 80Li₂S·20P₂S₅ Thin-Film Electrolytes Using Pulsed Laser Deposition. *J. Am. Ceram. Soc.* **2010**, *93* (3), 765-768.
3. Zhang, Y.; Chen, K.; Shen, Y.; Lin, Y.; Nan, C.-W., Synergistic effect of processing and composition x on conductivity of xLi₂S-(100-x)P₂S₅ electrolytes. *Solid State Ionics* **2017**, *305*, 1-6.
4. Tachez, M.; Malugani, J.-P.; Mercier, R.; Robert, G., Ionic conductivity of and phase transition in lithium thiophosphate Li₃PS₄. *Solid State Ionics* **1984**, *14* (3), 181-185.
5. Liu, Z.; Fu, W.; Payzant, E. A.; Yu, X.; Wu, Z.; Dudney, N. J.; Kiggans, J.; Hong, K.; Rondinone, A. J.; Liang, C., Anomalous High Ionic Conductivity of Nanoporous β -Li₃PS₄. *J. Am. Chem. Soc.* **2013**, *135* (3), 975-978.
6. Phuc, N. H. H.; Totani, M.; Morikawa, K.; Muto, H.; Matsuda, A., Preparation of Li₃PS₄ solid electrolyte using ethyl acetate as synthetic medium. *Solid State Ionics* **2016**, *288*, 240-243.
7. Whiteley, J. M.; Taynton, P.; Zhang, W.; Lee, S.-H., Ultra-thin Solid-State Li-Ion Electrolyte Membrane Facilitated by a Self-Healing Polymer Matrix. *Adv. Mater.* **2015**, *27* (43), 6922-6927.
8. Yamada, T.; Ito, S.; Omoda, R.; Watanabe, T.; Aihara, Y.; Agostini, M.; Ulissi, U.; Hassoun, J.; Scrosati, B., All Solid-State Lithium–Sulfur Battery Using a Glass-Type P₂S₅–Li₂S Electrolyte: Benefits on Anode Kinetics. *J. Electrochem. Soc.* **2015**, *162* (4), A646-A651.